

## Deformation Modes and Dual Stress Resultants of Spatial Beam Elements in Large Deflection Multibody System Analyses

**J. B. Jonker\***, **J. P. Meijaard#**

\* Laboratory of Mechanical Automation and Mechatronics, Faculty of Engineering Technology  
University of Twente  
P.O.Box 217, NL-7500 AE Enschede, The Netherlands  
j.b.jonker@utwente.nl

# Olton Engineering Consultancy  
Deurningerstraat 7-101, NL-7514 BC Enschede, The Netherlands  
j.p.meijaard@olton.nl

### ABSTRACT

A beam finite element formulation for large deflection problems in the analysis of flexible multibody systems has been proposed. In this formulation, a set of independent deformation modes are defined for each element that do not change if the element is subjected to rigid body motions. The paper examines the applicability of this deformation mode formulation for a shear-deformable three-dimensional Timoshenko-like beam model. In particular, the influence of the second-order terms in the expressions for the deformation modes on the results is shown. Some numerical examples including large deflections are presented and discussed in order to illustrate their effect on the accuracy and rate of convergence. Comparisons are made with analytical solutions of the large deflection of a cantilever beam and with numerical results obtained with the absolute nodal coordinate and geometrically exact beam formulations of a 45 degree cantilever bend. Finally, the vibration mode frequencies and buckling loads of a simple parallel leaf spring guidance subject to misalignment are analysed.

### 1 INTRODUCTION

Finite element models for flexible beams in a multibody system analysis can be formulated using either a one-dimensional continuum description with strain measures described with respect to a global reference frame (inertial frame approach), or on the basis of linear beam theories (i.e. Euler–Bernoulli as well as Timoshenko theories) in a local, co-rotational reference frame (moving frame approach). Articles by Reissner [20] and Simo and Vu-Quoc [22] provided a foundation for the development of a non-linear beam theory that is known as geometrically exact beam theory for finite rotations and deformations; see e.g. Géradin and Cardona [10]. The beam deformation is described with respect to an inertial reference frame. In this way large deformations are accurately represented as this formulation incorporates finite strain measures which are valid for arbitrary large displacements and rotations. This formulation has the advantage of accounting for non-linear effects due to deformation and, therefore, it can be used to study stability (buckling) and other problems where coupling between axial forces and bending and torsion deformations are of importance. However, a critical question in deriving finite element approximations based on the geometrically exact beam theory is the interpolation of finite rotations which can lead to lack of frame-invariance as described in [14, 21]. Because of the difficulties associated with the interpolation of finite rotations, so-called rotationless formulations have been developed, for example, the absolute nodal coordinate formulation as proposed by Yakoub and Shabana [24]. In this finite element formulation, nodal displacements and slope degrees of freedom are used for the interpolation of the displacement field of beam elements. Using absolute coordinates allows for large deformations and preserves an accurate description of rigid body motion. However, the use of global displacements and slopes as nodal coordinates results in a large number of nodal degrees of freedom. For example, a spatial beam element contains 24 nodal degrees of freedom; this is twice the number of nodal degrees of freedom compared with a conventional two-noded beam element.

In the co-rotational frame approach a local or co-rotational frame is attached to each flexible beam element. The motion of the element relative to this frame is approximately due only to the deformation motion of the

element. If the element size is chosen sufficiently small the deformations may be assumed to be small as well so linear beam theory can be used to compute the elastic displacements. It should be noted that the co-rotational formulation relies on the small deformation assumption in order to distinguish rigid body modes from deformation modes. Co-rotational finite element formulations for straight beams were first presented by Belytschko and Glaum [4] and have been applied for non-linear dynamic analyses of beam structures and mechanisms by Iura and Atluri [13], Elkaranshaw and Dokainish [9], Behdinan et al. [3], Hsiao et al. [12] and others. When modelling a flexible multibody system with elastic and rigid bodies, conventional co-rotational formulations treat rigid bodies in the same way as elastic bodies with large stiffness. Thus they are not able to model rigid body dynamics exactly yielding a less efficient formulation regarding computational time and eliminating high frequency modes of deformation.

Co-rotational formulations have much in common with the "natural mode approach" of Argyris et al. [1] and the "deformation mode formulation" of Besseling [5], published in the early 1960s. These two approaches refer to the use of deformation modes for the description of both deformation and rigid body motion of the element and allow for the development of a finite element based formulation for rigid-flexible multibody system analysis. This particular finite element description has been adopted to derive a beam finite element formulation for rigid-flexible multibody system analysis [15]. It is based on a beam model developed by Besseling [6, 7] for stability and post-buckling analysis of structures. In the original description, Euler angles were used to parametrize global nodal rotations. Van der Werff and Jonker [23] introduced a description including Euler parameters which is more appropriate for computations in multibody system codes and made possible an implementation in the program SPACAR [16]. For each beam element a set of independent deformation modes are defined that are invariant under arbitrary rigid body motions of the element. The deformation modes are characterized by deformation mode coordinates, the so-called generalized deformations, which are expressed as analytical functions of the absolute nodal coordinates, in a co-rotational context, i.e. the displacement field associated with each deformation mode is defined in its own co-rotational frame. The deformation functions include the specification of rigid body motions as displacements for which the generalized deformations are zero. Flexible beam elements are modelled by allowing non-zero deformations. Then constitutive equations relating generalized deformations and generalized stress-resultants have to be specified. The derivation of the element stiffness matrix is based on a discretization of the elastic line of a three-dimensional Timoshenko beam model in the local co-rotational frame for the undeformed configuration. A consistent mass matrix is derived using a discretization of the elastic line in the inertial frame [15, 18]. This formulation combines the advantages of the inertial frame approach (derivation of the inertia forces in terms of absolute nodal velocities and accelerations) and the co-rotational approach (application of linear beam theories in the derivation of the stiffness matrix). With this formulation, large deflection problems can be solved accurately as long as the element size is chosen sufficiently small, such that the generalized deformations remain small and linear relations between generalized stress resultants and generalized deformations are valid. However, when dynamic problems are considered, it is important that one is able to obtain sufficiently accurate solutions with a relatively small number of elements even when large deflections are considered. Decreasing the size of the elements increases, besides the number of degrees of freedom, the largest eigenfrequency in the system and reduces the allowed step size in explicit integration methods. Therefore the inclusion of second-order terms [18] in the description of the stiffness properties of the element could be valuable. These terms are also important for a proper representation of the geometric stiffness matrix which is necessary for the analysis of structural instability. In the present paper the effects of these second-order terms on the accuracy and rate of convergence of the numerical solutions are studied. Comparisons are made with analytical solutions of a large deformation cantilever beam [11] and with numerical results obtained with the absolute nodal coordinate and geometrically exact beam formulations of a 45 degree cantilever bend [21]. Finally, the vibration mode frequencies and buckling modes of a simple parallel leaf spring guidance subject to misalignment [19] are analysed.

## 2 FINITE-ELEMENT DESCRIPTION

### 2.1 Nodal base vectors and deformation modes

Figure 1 shows a spatial beam element in a global coordinate system  $Oxyz$ . The configuration of the element is determined by the position vectors  $\boldsymbol{x}^p$  and  $\boldsymbol{x}^q$  of the nodes at the ends and the angular orientations

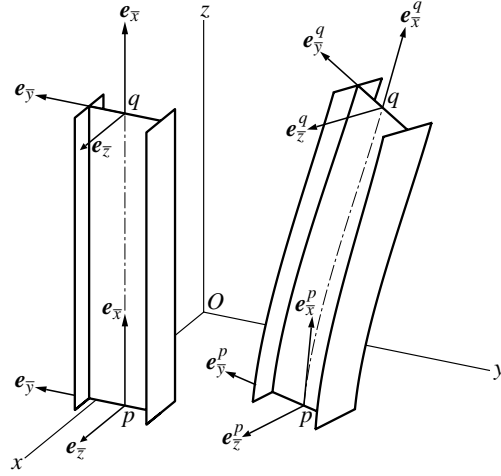


**Figure 1.** Beam element, reference and deformed state.

of orthonormal triads  $(e_x^p, e_y^p, e_z^p)$  and  $(e_x^q, e_y^q, e_z^q)$  rigidly attached to each end point. The rotational part of the motion of the flexible beam is determined by the rotations of the triads, which are described by rotation matrices  $\mathbf{R}^p$  and  $\mathbf{R}^q$  of the nodes,

$$\begin{aligned} e_x^p &= \mathbf{R}^p e_x; & e_x^q &= \mathbf{R}^q e_x; \\ e_y^p &= \mathbf{R}^p e_y; & e_y^q &= \mathbf{R}^q e_y; \\ e_z^p &= \mathbf{R}^p e_z; & e_z^q &= \mathbf{R}^q e_z. \end{aligned} \quad (1)$$

The nodal coordinates of the spatial beam element are the six Cartesian coordinates representing the vectors  $\mathbf{x}^p$  and  $\mathbf{x}^q$  and the rotation parameters representing the rotation matrices  $\mathbf{R}^p$  and  $\mathbf{R}^q$ ; if a redundant parametrization for the rotations is used, only six of them are independent. Therefore, as the beam has six degrees of freedom as a rigid-body, six independent deformation modes, specified by a set of deformation coordinates  $\varepsilon_i$ , can be expressed as analytical functions of the independent nodal coordinates,

$$\varepsilon_i = \mathcal{D}_i(x_k); \quad i = 1, \dots, 6; \quad k = 1, \dots, 12. \quad (2)$$

The conditions  $\varepsilon_i = 0$  impose rigidity on the element. Expressions for these deformation modes are [17, 18, 19]:

$$\begin{aligned} \varepsilon_1 &= \bar{\varepsilon}_1 + (2\bar{\varepsilon}_3^2 + \bar{\varepsilon}_3\bar{\varepsilon}_4 + 2\bar{\varepsilon}_4^2 + 2\bar{\varepsilon}_5^2 + \bar{\varepsilon}_5\bar{\varepsilon}_6 + 2\bar{\varepsilon}_6^2)/(30l_0) + c_t\bar{\varepsilon}_2^2/(2l_0^3), & (\text{elongation}) \\ \varepsilon_2 &= \bar{\varepsilon}_2 + (-\bar{\varepsilon}_3\bar{\varepsilon}_6 + \bar{\varepsilon}_4\bar{\varepsilon}_5)/l_0, & (\text{torsion}) \\ \varepsilon_3 &= \bar{\varepsilon}_3 + \bar{\varepsilon}_2(\bar{\varepsilon}_5 + \bar{\varepsilon}_6)/(6l_0), & (\text{bending in } xz\text{-plane}) \\ \varepsilon_4 &= \bar{\varepsilon}_4 - \bar{\varepsilon}_2(\bar{\varepsilon}_5 + \bar{\varepsilon}_6)/(6l_0), & \\ \varepsilon_5 &= \bar{\varepsilon}_5 - \bar{\varepsilon}_2(\bar{\varepsilon}_3 + \bar{\varepsilon}_4)/(6l_0), & (\text{bending in } xy\text{-plane}) \\ \varepsilon_6 &= \bar{\varepsilon}_6 + \bar{\varepsilon}_2(\bar{\varepsilon}_3 + \bar{\varepsilon}_4)/(6l_0), & \end{aligned} \quad (3)$$

with the basic deformation modes

$$\begin{aligned} \bar{\varepsilon}_1 &= l - l_0, \\ \bar{\varepsilon}_2 &= l_0(e_z^p \cdot e_y^q - e_y^p \cdot e_z^q)/2, \\ \bar{\varepsilon}_3 &= -l_0 \mathbf{e}_l \cdot \mathbf{e}_z^p, \\ \bar{\varepsilon}_4 &= l_0 \mathbf{e}_l \cdot \mathbf{e}_z^q, \\ \bar{\varepsilon}_5 &= l_0 \mathbf{e}_l \cdot \mathbf{e}_y^p, \\ \bar{\varepsilon}_6 &= -l_0 \mathbf{e}_l \cdot \mathbf{e}_y^q, \end{aligned} \quad (4)$$

where  $l_0$  is the reference length of the element,  $\mathbf{l} = \mathbf{x}^q - \mathbf{x}^p$  is the vector from node  $p$  to node  $q$ ,  $l = \|\mathbf{l}\|$  is the distance between the nodes and  $\mathbf{e}_l = (\mathbf{x}^q - \mathbf{x}^p)/l$  is the unit vector directed from node  $p$  to node  $q$ . The

first deformation coordinate,  $\varepsilon_1$ , describes the elongation of the beam, the second one,  $\varepsilon_2$ , the torsion and the other four describe beam deflections along the local  $\bar{y}$ - and  $\bar{z}$ -axes at the nodes. The physical dimension of all generalized deformations is length. The element accounts for geometrically non-linear effects due to the interaction between the deformation modes. Consequently, the expression for the beam elongation  $\varepsilon_1$  contains additional terms which take into account the additional elongation of the beam axis caused by torsion and bending. The additional terms in  $\varepsilon_2$  measure extra torsion of the beam caused by its bending. The term with the torsional constant  $c_t$  accounts for torsion–elongation coupling [19]. Furthermore, the additional terms in the expressions for the bending deformations account for the effect of asymmetrical bending caused by a twist of the beam.

## 2.2 Generalized stress resultants

Let us consider an equilibrium force system defined by the nodal forces  $\mathbf{F}^p$  and  $\mathbf{F}^q$  and the nodal moments  $\mathbf{T}^p$  and  $\mathbf{T}^q$  applied at the nodal points  $p$  and  $q$  of the free element, which are placed in a vector of element nodal forces,

$$\mathbf{f} = [\mathbf{F}^{pT}, \mathbf{T}^{pT}, \mathbf{F}^{qT}, \mathbf{T}^{qT}]^T. \quad (5)$$

This is the general case if all distributed forces, including inertia terms, are replaced by equivalent nodal forces. Furthermore, we consider virtual variations of the nodal displacements,  $\delta \mathbf{x}^p$  and  $\delta \mathbf{x}^q$ , and virtual rotations  $\delta \varphi^p$  and  $\delta \varphi^q$ , which are represented by a vector of virtual nodal displacements,

$$\delta \mathbf{u} = [\delta \mathbf{x}^{pT}, \delta \varphi^{pT}, \delta \mathbf{x}^{qT}, \delta \varphi^{qT}]^T. \quad (6)$$

Virtual variations of the generalized deformations depend on these virtual nodal displacements through the compatibility relations (2) which can be expressed as

$$\delta \varepsilon_i = D_{il} \delta u_l \quad (7)$$

Generalized stress resultants,  $\sigma_i$ , are defined to be energetically dual to the generalized deformations. According to the principle of virtual work, the element will be in a state of equilibrium if

$$\sigma_i \delta \varepsilon_i = f_k \delta u_k, \quad \text{or} \quad \boldsymbol{\sigma}^T \delta \boldsymbol{\varepsilon} = \mathbf{f}^T \delta \mathbf{u} \quad (8)$$

holds for all  $\delta \mathbf{u}$  and  $\delta \boldsymbol{\varepsilon}$  depending on  $\delta \mathbf{u}$  by the relations (7). This yields the equilibrium equations

$$f_l = D_{il} \sigma_i. \quad (9)$$

The matrix  $D_{il}$  relates the variations of the generalized deformations  $\delta \varepsilon_i$  to the virtual displacements  $\delta u_l$ . The stress resultants  $\sigma_1$ ,  $l_0 \sigma_2$  and  $l_0 \sigma_3 - l_0 \sigma_6$  can be associated with the well known beam quantities as normal force, twisting moment and four bending moments. Note that  $\sigma_2$  for torsion corresponds to a pair of moments at the nodes in opposite directions that are approximately along the beam axis. It can be easily shown [17] that equilibrium is obtained for arbitrary large deformations and rigid body displacements. This can be attributed to the invariance of the generalized deformations under rigid body displacements, so rigid body displacements leaving the generalized deformations unchanged can be described.

## 2.3 The stiffness matrix

In the present finite-element method, the generalized deformations and dual generalized stress resultants move with the element as it is translated and rotated. Consequently, the linear beam theory based on the elastic line concept can be used for deriving relations between generalized strains and generalized stress resultants, provided that the element size is chosen sufficiently small and the physical deformations remain small. The generalized stress resultants and generalized deformations are related by linear elasticity equations

$$\sigma_i = S_{ij} \varepsilon_j, \quad \text{or} \quad \boldsymbol{\sigma} = \mathbf{S} \boldsymbol{\varepsilon}, \quad (10)$$

where  $\mathbf{S}$  is a symmetric matrix containing the elasticity constants. The components of  $\mathbf{S}$  are calculated by means of a cubic polynomial interpolation for the lateral displacement from the line connecting the nodal points, incorporating the shear effects. This is the exact linear displacement field for the case when the beam

is loaded by equilibrium forces and moments at its nodes. The global position vector  $\mathbf{x}(\xi)$  for a point with material coordinate  $s = \xi l_0$  can be expressed as a vectorial sum of a point on the line connecting the nodes and the lateral deflection expressed as the linear combination of four components linear in the deformation coordinates  $\varepsilon_3, \varepsilon_4, \varepsilon_5$  and  $\varepsilon_6$ , respectively [15]

$$\mathbf{x}(\xi) = (1 - \xi)\mathbf{x}^p + \xi\mathbf{x}^q + \varepsilon_3 w^p(\xi) \mathbf{e}_z^p + \varepsilon_4 w^q(\xi) \mathbf{e}_z^q + \varepsilon_5 v^p(\xi) \mathbf{e}_y^p + \varepsilon_6 v^q(\xi) \mathbf{e}_y^q. \quad (11)$$

The shape functions corresponding to the bending deformations are

$$w^p(\xi) = \frac{1}{1 + \Phi_z} \left[ \xi^3 - 2\xi^2 + \xi + \frac{1}{2} \Phi_z (-\xi^2 + \xi) \right], \quad (12)$$

$$w^q(\xi) = \frac{1}{1 + \Phi_z} \left[ -\xi^3 + \xi^2 + \frac{1}{2} \Phi_z (-\xi^2 + \xi) \right], \quad (13)$$

$$v^p(\xi) = -\frac{1}{1 + \Phi_y} \left[ \xi^3 - 2\xi^2 + \xi + \frac{1}{2} \Phi_y (-\xi^2 + \xi) \right], \quad (14)$$

$$v^q(\xi) = -\frac{1}{1 + \Phi_y} \left[ -\xi^3 + \xi^2 + \frac{1}{2} \Phi_y (-\xi^2 + \xi) \right], \quad (15)$$

with the shear factors

$$\Phi_z = \frac{12EI_y}{k_z G A l_0^2}, \quad \Phi_y = \frac{12EI_z}{k_y G A l_0^2}. \quad (16)$$

Equation (11) shows that the displacement field associated with the bending deformation of the beam element is described with respect to four co-rotational frames that coincide with the orthogonal triads of unit vectors,  $(\mathbf{e}_x, \mathbf{e}_y, \mathbf{e}_z)$  at the nodes  $p$  and  $q$ . In the undeflected state, these triads coincide with the axis  $pq$  and the principal axes of the cross-section, so Eq. (11) simplifies to the form

$$\mathbf{x}(\xi) = (1 - \xi)\mathbf{x}^p + \xi\mathbf{x}^q + [\varepsilon_3 w^p(\xi) + \varepsilon_4 w^q(\xi)] \mathbf{e}_z + [\varepsilon_5 v^p(\xi) + \varepsilon_6 v^q(\xi)] \mathbf{e}_y. \quad (17)$$

If the beam can shear, the rotations cannot directly be derived from the deflections, but are interpolated independently; the small rotations  $\varphi$  are

$$l_0 \varphi = \xi \varepsilon_2 \mathbf{e}_x + [\varepsilon_3 \varphi_y^p(\xi) + \varepsilon_4 \varphi_y^q(\xi)] \mathbf{e}_y + [\varepsilon_5 \varphi_z^p(\xi) + \varepsilon_6 \varphi_z^q(\xi)] \mathbf{e}_z \quad (18)$$

with the shape functions

$$\varphi_y^p(\xi) = \frac{1}{1 + \Phi_z} \left[ -3\xi^2 + 4\xi - 1 + \Phi_z (\xi - 1) \right], \quad (19)$$

$$\varphi_y^q(\xi) = \frac{1}{1 + \Phi_z} \left[ 3\xi^2 - 2\xi + \Phi_z \xi \right], \quad (20)$$

$$\varphi_z^p(\xi) = \frac{1}{1 + \Phi_y} \left[ -3\xi^2 + 4\xi - 1 + \Phi_y (\xi - 1) \right], \quad (21)$$

$$\varphi_z^q(\xi) = \frac{1}{1 + \Phi_y} \left[ 3\xi^2 - 2\xi + \Phi_y \xi \right]. \quad (22)$$

By virtue of these displacement and rotation distributions, the elasticity coefficients of the stiffness matrix  $\mathbf{S}$  are expressed as

$$\mathbf{S} = \text{diag}\{S_1, S_2, \mathbf{S}_3, \mathbf{S}_4\}, \quad (23)$$

$$S_1 = \frac{EA}{l_0}, \quad S_2 = \frac{k_x G I_p}{l_0^3},$$

$$\mathbf{S}_3 = \frac{EI_y}{(1 + \Phi_z) l_0^3} \begin{bmatrix} 4 + \Phi_z & -2 + \Phi_z \\ -2 + \Phi_z & 4 + \Phi_z \end{bmatrix}, \quad (24)$$

$$\mathbf{S}_4 = \frac{EI_z}{(1 + \Phi_y) l_0^3} \begin{bmatrix} 4 + \Phi_y & -2 + \Phi_y \\ -2 + \Phi_y & 4 + \Phi_y \end{bmatrix}.$$

If the beam is loaded by relatively large forces in comparison with the buckling load, the influence of geometric non-linearities has to be taken into account. With the inclusion of the second-order terms in the definitions of the generalized deformations of Eq. (3) the linear relations with the dual generalized stress resultants are retained, which has the advantage that the separation of deformations associated with high stiffness from deformations associated with low stiffness is retained. We refer to [18] for a more detailed discussion.

## 2.4 Consistent mass matrix

In order to obtain a consistent mass matrix and the corresponding convective inertia terms, an interpolation of the position of the elastic line has to be made. With cubic polynomial interpolation for the bending deformations that incorporate parameters that account for the effect of shear as well, the global position vector  $\mathbf{x}(\xi)$  of a point with material coordinate  $s = l_0\xi$  in the deflected state of the beam element can be expressed as in Eq. (11). This interpolation leads to a complex expression for the inertia forces, and so a modified interpolation was proposed [18] as

$$\mathbf{x}(\xi) = \mathbf{x}^p(2\xi^3 - 3\xi^2 + 1) + l_0\mathbf{e}_x^p(\xi^3 - 2\xi^2 + \xi) + \mathbf{x}^q(-2\xi^3 + 3\xi^2) + l_0\mathbf{e}_x^q(\xi^3 - \xi^2). \quad (25)$$

Eq. (25) can be derived from Eq. (11) by neglecting the shear factors (16), the axial strain and the difference between  $l_0$  and  $l$ . The velocity and acceleration distribution can be found by taking time derivatives as

$$\dot{\mathbf{x}}(\xi) = \dot{\mathbf{x}}^p(2\xi^3 - 3\xi^2 + 1) + l_0\mathbf{B}^p\dot{\vartheta}^p(\xi^3 - 2\xi^2 + \xi) + \dot{\mathbf{x}}^q(-2\xi^3 + 3\xi^2) + l_0\mathbf{B}^q\dot{\vartheta}^q(\xi^3 - \xi^2) \quad (26)$$

and

$$\begin{aligned} \ddot{\mathbf{x}}(\xi) = & \ddot{\mathbf{x}}^p(2\xi^3 - 3\xi^2 + 1) + l_0(\mathbf{B}^p\ddot{\vartheta}^p + \dot{\mathbf{B}}^p\dot{\vartheta}^p)(\xi^3 - 2\xi^2 + \xi) \\ & + \ddot{\mathbf{x}}^q(-2\xi^3 + 3\xi^2) + l_0(\mathbf{B}^q\ddot{\vartheta}^q + \dot{\mathbf{B}}^q\dot{\vartheta}^q)(\xi^3 - \xi^2), \end{aligned} \quad (27)$$

where

$$\mathbf{B}^p = \frac{\partial \mathbf{e}_x^p}{\partial \vartheta^p}, \quad \mathbf{B}^q = \frac{\partial \mathbf{e}_x^q}{\partial \vartheta^q}, \quad \dot{\mathbf{B}}^p = \frac{\partial \mathbf{B}^p}{\partial \vartheta^p} \dot{\vartheta}^p, \quad \dot{\mathbf{B}}^q = \frac{\partial \mathbf{B}^q}{\partial \vartheta^q} \dot{\vartheta}^q. \quad (28)$$

The virtual work due to the inertia terms is

$$-\rho A l_0 \int_0^1 \delta \mathbf{x}^T \ddot{\mathbf{x}} d\xi = -\delta \mathbf{x}^{eT} [\mathbf{M}_{\text{in}} \ddot{\mathbf{x}}^e - \mathbf{f}_{\text{in}}] \quad (29)$$

with the mass matrix

$$\mathbf{M}_{\text{in}} = \frac{\rho A l_0}{420} \begin{bmatrix} 156\mathbf{I} & 22l_0\mathbf{B}^p & 54\mathbf{I} & -13l_0\mathbf{B}^q \\ 22l_0\mathbf{B}^{pT} & 4l_0^2\mathbf{B}^{pT}\mathbf{B}^p & 13l_0\mathbf{B}^{pT} & -3l_0^2\mathbf{B}^{pT}\mathbf{B}^q \\ 54\mathbf{I} & 13l_0\mathbf{B}^p & 156\mathbf{I} & -22l_0\mathbf{B}^q \\ -13l_0\mathbf{B}^{qT} & -3l_0^2\mathbf{B}^{qT}\mathbf{B}^p & -22l_0\mathbf{B}^{qT} & 4l_0^2\mathbf{B}^{qT}\mathbf{B}^q \end{bmatrix} \quad (30)$$

and the convective terms

$$-\mathbf{f}_{\text{in}} = \frac{\rho A l_0}{420} \begin{bmatrix} 22l_0\dot{\mathbf{B}}^p\dot{\vartheta}^p - 13l_0\dot{\mathbf{B}}^q\dot{\vartheta}^q \\ 4l_0^2\mathbf{B}^{pT}\dot{\mathbf{B}}^p\dot{\vartheta}^p - 3l_0^2\mathbf{B}^{pT}\dot{\mathbf{B}}^q\dot{\vartheta}^q \\ 13l_0\dot{\mathbf{B}}^p\dot{\vartheta}^p - 22l_0\dot{\mathbf{B}}^q\dot{\vartheta}^q \\ -3l_0^2\mathbf{B}^{qT}\dot{\mathbf{B}}^p\dot{\vartheta}^p + 4l_0^2\mathbf{B}^{qT}\dot{\mathbf{B}}^q\dot{\vartheta}^q \end{bmatrix}, \quad (31)$$

where  $\rho$  is the specific mass of the beam material.

## 3 NUMERICAL SIMULATIONS

### 3.1 Cantilever beam loaded by a transverse force

As a first example, a cantilever beam loaded by a large transverse force is studied (Figure 2). This example was studied in [8] with the inclusion of shear and in [11] for the case without shear, which is also studied here to make a comparison. The beam has a length of  $L = 2$  m, a square cross-section with sides 0.1 m, Young's modulus  $E = 207$  GPa, and the load is chosen as  $F = 3EI/L^2$ , so the deflection would be equal to the length of the beam according to the linear theory.

Table 1 shows the tip displacements for different numbers of equal elements. The displacements in the second and third column have been obtained with the compound definitions for the generalized deformations of Eq. (3), while the displacements in the fourth and fifth column have been obtained with the basic definitions of Eq. (4). The row indicated by  $\infty$  is obtained by extrapolation. The observed rate of convergence is quadratic. This contrasts with the results obtained in [11] where a quartic rate of convergence was obtained, which can be attributed to the use of a full third-order polynomial interpolation for the displacements. The inclusion of the quadratic terms in the definitions for the generalized deformations gives a small improvement of the computed displacements.

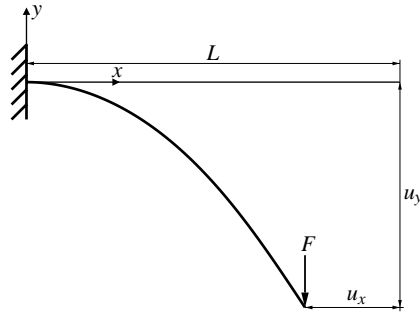


Figure 2. Cantilever beam loaded by a transverse force.

Table 1. Tip displacements;  $u_x$  and  $u_y$  are obtained with the inclusion of the quadratic terms in the strain definitions, whereas  $\bar{u}_x$  and  $\bar{u}_y$  lack these terms.

Elements	$u_x$	$u_y$	$\bar{u}_x$	$\bar{u}_y$
1	0.901066644798	1.521303825634	no convergence	no convergence
2	0.574104241718	1.276622418852	0.575337548831	1.316822924102
4	0.523295236718	1.223753236062	0.521435397690	1.230944822127
8	0.512120512808	1.211296300191	0.511573006267	1.212950648542
16	0.509426561728	1.208249238659	0.509285242228	1.208654613824
32	0.508759212038	1.207491902527	0.508723614476	1.207592744726
64	0.508592755920	1.207302847936	0.508583839922	1.207328027289
128	0.508551165641	1.207255601727	0.508548935607	1.207261894619
$\infty$	0.508537302215	1.207239852991	0.508537234168	1.207239851396
$\infty$ [11]	0.508537304325	1.207239854550		

### 3.2 Cantilever beam initially curved to a 45 degree arc

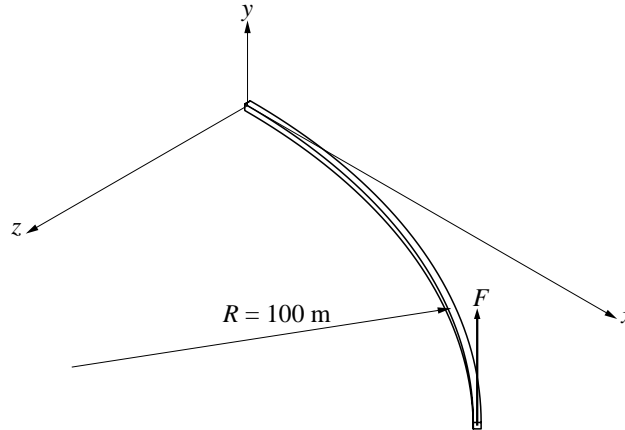


Figure 3. Cantilever beam initially curved to a 45 degree arc in the undeformed configuration.

An example, originally proposed by Bathe [2], which has recently been considered in Romero's paper [21], consists of a cantilever beam initially curved to an arc of radius 100 m over an angle of  $45^\circ$  in a horizontal plane (Fig. 3). The beam is loaded by a vertical tip force of 600 N, which is applied in four equal load increments. The properties of the beam are  $EA = 10 \times 10^6$  N,  $k_{\bar{y}}GA = k_{\bar{z}}GA = 5 \times 10^6$  N,  $k_{\bar{x}}GI_p = EI_{\bar{y}} = EI_{\bar{z}} = 1 \times 10^7/12$  Nm<sup>2</sup>. The beam is modelled by eight equal initially straight beam elements with the nodes on the centre line of the beam. The tip position predicted by the present deformation mode (DM)

formulation compared with results obtained in the original publication [2], results from a geometrically exact (GE) formulation [21], from an absolute nodal coordinate (ANC) formulation and from a co-rotational (CR) formulation [14] are listed in Table 2.

**Table 2.** Tip position (m) for the curved cantilever beam. Initial tip coordinates: (70.71, 0, 29.29)

	$F = 300 \text{ N}$			$F = 450 \text{ N}$			$F = 600 \text{ N}$		
	$r_x$	$r_y$	$r_z$	$r_x$	$r_y$	$r_z$	$r_x$	$r_y$	$r_z$
Bathe & Belourchi [2]	59.2	39.5	22.5	—	—	—	47.2	53.4	15.9
GE (8 elements)	58.61	40.35	22.21	52.05	48.59	18.49	46.98	53.50	15.69
GE (50 elements)	58.54	40.48	22.12	51.59	48.70	18.37	46.89	53.60	15.56
ANC (4 elements)	64.78	28.68	25.66	62.14	33.94	24.04	59.95	37.55	22.71
ANC (8 elements)	59.98	38.18	22.88	54.45	45.71	19.71	50.16	50.26	17.16
CR ([14], 8 el.)	—	—	—	—	—	—	46.97	53.73	15.62
DM (Eq. (4), 8 el.)	58.73	40.32	22.23	52.11	48.72	18.46	46.95	53.75	15.61
DM (Eq. (3), 8 el.)	58.71	40.27	22.24	52.10	48.63	18.48	46.94	53.64	15.64
DM (Eq. (3), 48 el.)	58.78	40.19	22.24	52.23	48.51	18.51	47.14	53.48	15.68

The results show that all methods provide accurate solutions with the exception of the ANC solutions. This is even clearer when we compare with ANC solutions having the same number of degrees of freedom, namely with ANC (4 elements) [21].

### 3.3 Parallel leaf-spring guidance

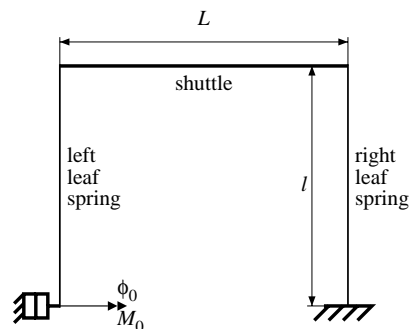


**Figure 4.** Parallel leaf spring guidance with adjustable misalignment.

A parallel leaf spring guidance is shown in Fig. 4. It consists of a guided body, the shuttle, supported by two leaf springs. The two leaf springs are equal and they are parallel in the reference configuration. The base of the left leaf spring is connected to a shaft, so a preload or a prescribed misalignment can be introduced. The stainless steel leaf springs have a thickness  $t = 0.2 \text{ mm}$ , a width  $b = 30 \text{ mm}$  and a length  $l = 100 \text{ mm}$ , and they are a distance  $L = 120 \text{ mm}$  apart. Further details of the model can be found in [19]. Ten spatial beam elements are used to model each leaf spring. The critical moment  $M_0$  for buckling is found to be  $0.30129 \text{ Nm}$  with the compound definition Eq. (3) and  $0.30361 \text{ Nm}$  with the basic definition Eq. (4). The difference is caused by the gravity load and the quadratic term with  $c_t$  in  $\varepsilon_1$ ; if gravity is omitted in the model, both formulations yield the same buckling load.

The first three natural frequencies as a function of the misalignment angle  $\phi_0$  are shown in Figure 5. The three eigenfrequencies drop considerably at the critical angle of about  $0.8 \text{ milliradians}$  at which bifurcation occurs. The difference between the two formulations is small at zero misalignment, then increases strongly near the critical angle, nearly to a ratio of one to two for the second natural frequency, and then decrease again. It can be observed that the difference for the second natural frequency remains large for angles larger than the critical angle.



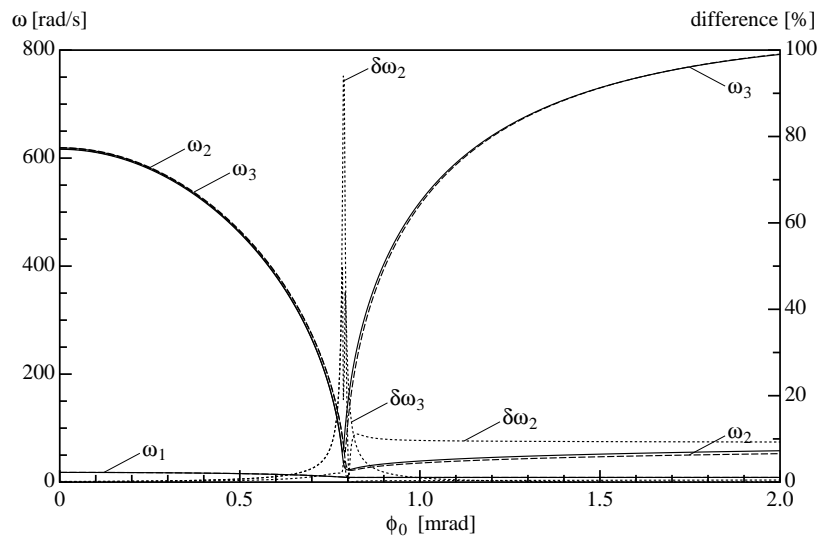


**Figure 5.** First three eigenfrequencies for varying misalignments. The solid lines are with the compound definition of Eq. (3) and the dashed lines are for the basic definitions of Eq. (4). The dotted lines show the relative difference  $\delta\omega_i$ , ( $i = 1, 2, 3$ ) between the eigenfrequencies.

#### 4 CONCLUSIONS

In the present paper we investigated the effect of second-order terms in the expressions for the deformation modes that account for geometric non-linearity. The influence of these second-order terms on the displacements is small, except for bifurcation points where the system behaviour changes drastically. However, the use of these terms does not lead to a considerable reduction in the number of elements needed to perform the analysis with the same accuracy. It is demonstrated, by comparison with available results in literature, that highly accurate solutions can be obtained with the present beam finite element formulation.

#### REFERENCES

- [1] Argyris, J.H.; Balmer, H.; Doltsinis, J.; Dunne, P.C.; Haase, M.; Kleiber, M.; Malejannakis, G.A.; Mlejnek, H.P.; Müller, M.; Scharpf, D.W.: *Finite Element Method – the Natural Approach*. Computer Methods in Applied Mechanics and Engineering, Vol. 17/18, pp. 1–106, 1979.
- [2] Bathe, K.-J.; Bolourchi, S.: *Large Displacement Analysis of Three-Dimensional Beam Structures*. International Journal for Numerical Methods in Engineering, Vol. 14, pp. 961–986, 1979.
- [3] Behdinan, K.; Stylianou, M.C.; Tabarrok, B.: *Co-rotational Dynamic Analysis of Flexible Beams*. Computer Methods in Applied Mechanics and Engineering, Vol. 54, pp. 151–161, 1998.
- [4] Belytschko, T.; Glaum, L.W.: *Application of Higher Order Corotational Stretch Theories to Non-Linear Finite Element Analysis*. Computers and Structures, Vol. 10, pp. 175–182, 1979.
- [5] Besseling, J.F.: *The Complete Analogy between the Matrix Equations and the Continuous Field Equations of Structural Analysis*. In F. Haus (Ed.) *International Symposium on Analogue and Digital Techniques Applied to Aeronautics*, Proceedings, pp. 298–305, Presses Académiques Européennes, Bruxelles, 1964.
- [6] Besseling, J.F.: *Derivatives of Deformation Parameters for Bar Elements and Their Use in Buckling and PostBuckling Analysis*. Computer Methods in Applied Mechanics and Engineering, Vol. 12, pp. 97–124, 1977.

- [7] Besseling, J.F.: Non-Linear Theory for Elastic Beams and Rods and its Finite Element Representation. *Computer Methods in Applied Mechanics and Engineering*, Vol. 31, pp. 205–220, 1982.
- [8] Dufva, K.E.; Sopanen, J.T.; Mikkola, A.M.: A Two-Dimensional Shear Deformable Beam Element Based on the Absolute Nodal Coordinate Formulation. *Journal of Sound and Vibration* Vol. 280, pp. 719–738, 2005.
- [9] Elkaranshaw, H.A.; Dokainish, M.A.: Corotational Finite Element Analysis of Planar Flexible Multibody Systems. *Computers and Structures*, Vol. 54, No. 5, pp. 881–890, 1995.
- [10] Géradin, M.; Cardona, A.: *Flexible Multibody Dynamics, a Finite Element Approach*. John Wiley and Sons, Chichester, 2001.
- [11] Gerstmayr, J.; Irschik, H.: On the Correct Representation of Bending and Axial Deformation in the Absolute Nodal Coordinate Formulation with an Elastic Line Approach. *Journal of Sound and Vibration*, Vol. 318, pp. 461–487, 2008.
- [12] Hsiao, K.M.; Lin, J.Y.; Lin, W.Y.: A Consistent Co-rotational Finite Element Formulation for Geometrically Nonlinear Dynamic Analysis of 3-D Beams. *Computer Methods in Applied Mechanics and Engineering*, Vol. 169, pp. 1–18, 1999.
- [13] Iura, M.; Atluri, S.N.: On a Consistent Theory, and Variational Formulation of Finitely Stretched and Rotated 3-D Space-Curved Beams. *Computational Mechanics*, Vol. 4, pp. 73–8, 1989.
- [14] Jelenić, G.; Crisfield, M.A.: Geometrically Exact 3D Beam Theory: Implementation of a Strain-Invariant Finite Element for Statics and Dynamics. *Computer Methods in Applied Mechanics and Engineering*, Vol. 171, pp. 141–171, 1999.
- [15] Jonker, J.B.: A Finite Element Dynamic Analysis of Flexible Spatial Mechanisms and Manipulators. *Computer Methods in Applied Mechanics and Engineering*, Vol. 76, pp. 17–40, 1989.
- [16] Jonker, J.B.; Meijaard, J.P.: SPACAR – Computer Program for Dynamic Analysis of Flexible Spatial Mechanisms and Manipulators. In W. Schiehlen (Ed.) *Multibody Systems Handbook*, pp. 123–143, Springer-Verlag, Berlin, 1990.
- [17] Jonker, J.B.; Meijaard, J.P.: Definition of Deformation Parameters for Beam Elements and Their Use in Flexible Multibody System Analysis. In K. Arczewski, J. Frączek, M. Wojtyra (Eds.) *Multibody Dynamics 2009, ECCOMAS Thematic Conference*, Warsaw, 2009.
- [18] Meijaard, J.P.: Validation of Flexible Beam Elements in Dynamics Programs. *Nonlinear Dynamics*, Vol. 9, No. 1–2, pp. 21–36, 1996.
- [19] Meijaard, J.P.; Brouwer, D.M.; Jonker, J.B.: Analytical and Experimental Investigation of a Parallel Leaf Spring Guidance. *Multibody System Dynamics*, Vol. 23, No. 1, pp. 77–97, 2010.
- [20] Reissner, E.: On One-dimensional Finite-Strain Beam Theory: The Plane Problem. *Journal of Applied Mathematics and Physics (ZAMP)*, Vol. 23, pp. 795–804, 1972.
- [21] Romero, I.: A Comparison of Finite Elements for Non-Linear Beams: the Absolute Nodal Coordinate and Geometrically Exact Formulations. *Multibody System Dynamics*, Vol. 20, No. 1, pp. 51–68, 2008.
- [22] Simo, J.C.; Vu-Quoc, L.: On the Dynamics of Flexible Beams under Large Overall Motions – the Plane Case: part I and II. *Journal of Applied Mechanics*, Vol. 53, pp. 849–863, 1986.
- [23] Werff, K. van der; Jonker, J.B.: Dynamics of flexible mechanisms. In E.J. Haug (Ed.) *Proceedings of Computer Aided Analysis and Optimization of Mechanical System Dynamics*, pp. 381–400, Springer-Verlag, Berlin, 1984.
- [24] Yakoub, R.Y.; Shabana, A.A.: Three Dimensional Absolute Nodal Coordinate Formulation for Beam Elements: Implementation and Applications. *ASME Journal of Mechanical Design*, Vol. 123, pp. 614–621, 2001.